Si Nanoribbons on Ag(110) Studied by Grazing-Incidence X-Ray Diffraction, Scanning Tunneling Microscopy, and Density-Functional Theory: Evidence of a Pentamer Chain Structure

Geoffroy Prévot, Conor Hogan, Thomas Leoni, Romain Bernard, Eric Moyen, Laurence Masson

Si nanoribbons on Ag(110) studied by grazing incidence x-ray diffraction, scanning tunneling microscopy, and density-functional theory : evidence of a pentamer chain structure

Geoffroy Prévot[1,†], Conor Hogan[2], Thomas Leoni[3], Romain Bernard[1], Eric Moyen[3,§], Laurence Masson[3,†]

[1]*Sorbonne Universités, UPMC Univ Paris 06, CNRS-UMR 7588, Institut des NanoSciences de Paris, F-75005, Paris, France*

[2]*CNR-Istituto di Struttura della Materia, Via Fosso del Cavaliere 100, 00133 Rome, Italy*

and Dipartimento di Fisica, Università di Rome "Tor Vergata", Via della Ricerca Scientifica 1, 00133 Rome, Italy

[3]*Aix Marseille Univ, CNRS, CINaM , Marseille, France*

Corresponding Author
† e-mail : prevot@insp.jussieu.fr, masson@cinam.univ-mrs.fr

Present Addresses
§ Department of Energy Science (DOES), Sungkyunkwan University , N center, Jangan-gu, Gyeonggi-do, Suwon 16419, South Korea

Supplemental Material

In this supplemental material are presented a DFT energy diagram including van der Waals corrections, some details relative to STM and GIXD experiments performed on Si/Ag(110) nanoribbons grown at 460 K, and a table summarizing the success of different structural models.

DFT-GGA-vdW calculations

Fig. S1 shows the surface formation energy of the different Si/Ag(110) structures computed using GGA-PBE with van der Waals corrections. The only significant variation with respect to LDA calculations (see Fig. 1 in the main document) is the shift of the surface energy for the honeycomb model towards lower values. However, the chain of pentamers is the most stable monolayer structure in a wide range of chemical potentials.

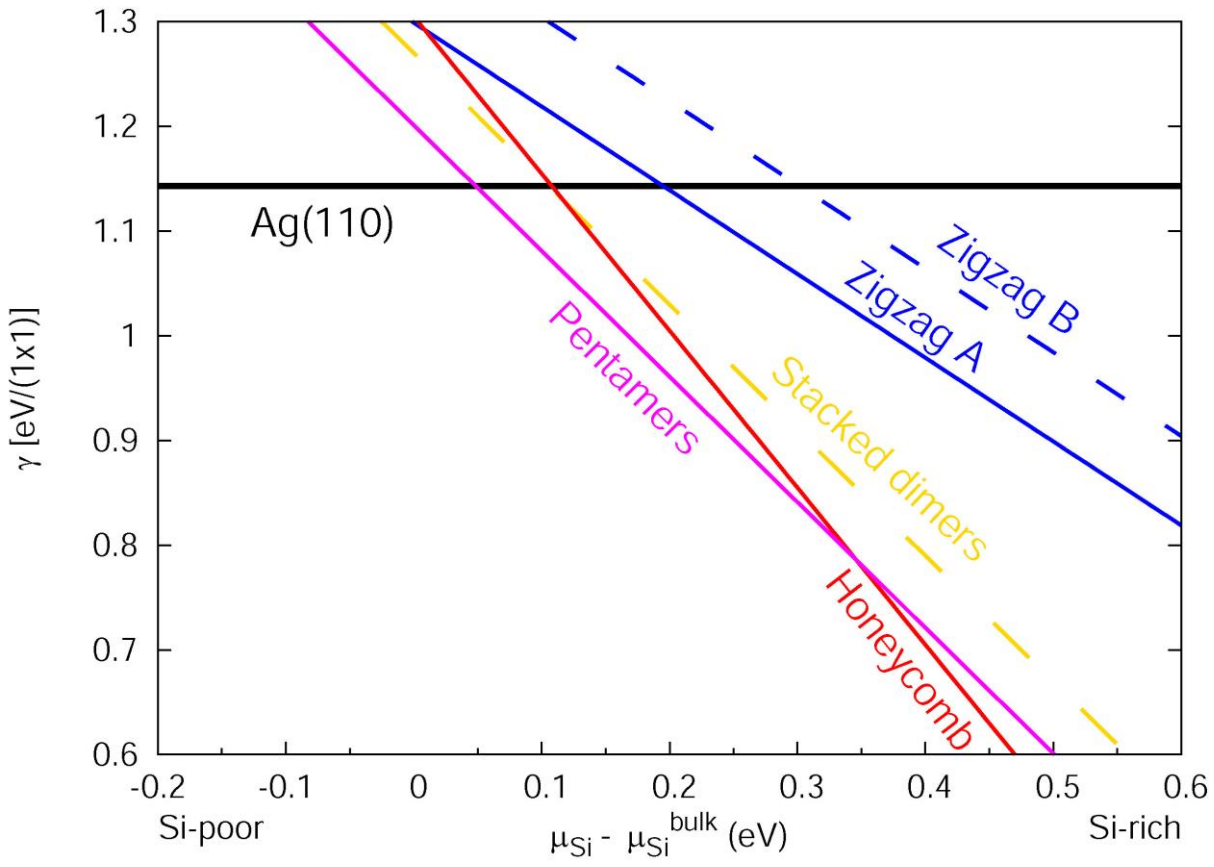

Figure S1. Surface formation energies for the main structural models considered in this work, as computed using GGA-PBE with van der Waals corrections.

STM experiments

Fig. S2 shows STM images of the Si nanoribbons (NRs) grown on Ag(110) taken using standard measurement conditions following growth at 460K, below 1 ML coverage. At this temperature, Si self-organized in ordered domains of double NRs, separated with bare surface regions. A few 0.8 nm-wide single NRs also form. These images are consistent with those previously published on this system.

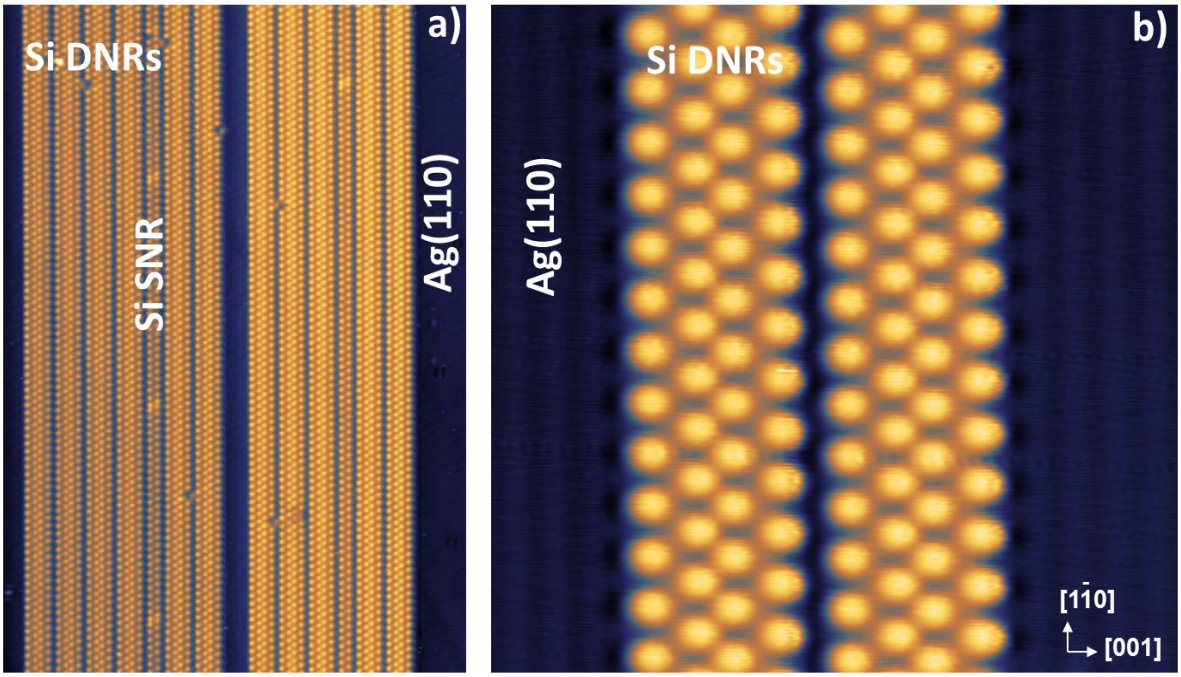

Figure S2. STM images of Si single nanoribbons (SNRs) and double nanoribbons (DNRs) below completion of the Si monolayer. a) (47×33 nm^2) I = 200 pA, V_{sample}= 140 mV. b) (7.5×6.5 nm^2) I = 480 pA, V_{sample}= 40 mV. The Ag atomic rows along [1$\bar{1}$0] are visible.

GIXD experiments

In Fig. S3 is presented a scan in the k direction for k=0 and l=0.05. In addition to the crystal truncation rod at h=1, peaks at h=0.6, 0.8, 1.4, 1.6 are clearly visible, with a FWHM of 0.033, which corresponds to a mean domain size of ~12 nm in the x direction. The scans are much narrow along the k direction, due to the highly anisotropic aspect ratio of the nanoribbons. In that case, the FWHM is given by the apparatus resolution.

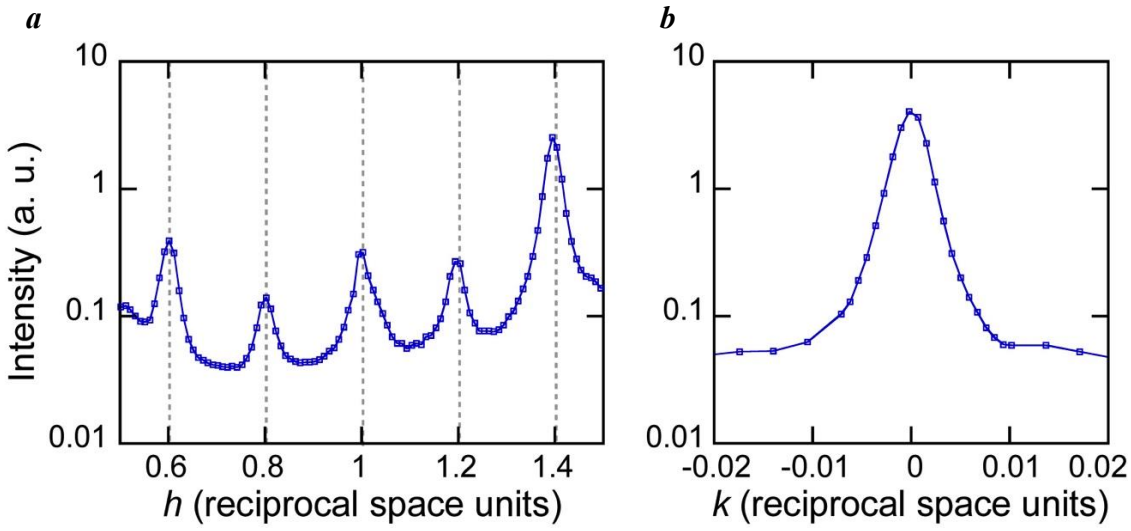

Figure S3. X-ray diffraction signal from the surface after 1ML Si deposition at 460 K. a) h-scan for $k = 0$ and $l = 0.05$. b) k-scan for $l = 0.05$ and $h = 1.4$.

Structure factor measurements were done by performing standard rocking scans with a point detector. Voigt curves were used for integrating the profile of the rocking scans and deriving the diffracted intensity. The standard instrumental correction was applied to the structure factors for taking into account the geometry of the diffractometer, the sample dimensions, and the width of the rods along h and k. [1] The experimental uncertainties σ_{exp} take into account both statistical uncertainties and systematic errors due, for example, to misalignment, and estimated in the range of 10%.

In Fig. S4 is presented the comparison between the experimental structure factors measured and the theoretical structure factors derived from the stacked dimers model. The agreement is

very poor. In particular, it is not possible to reproduce the high intensity of the $(1.4\,0\,L)$ row without taking into account a missing row reconstruction of the Ag(110) substrate.

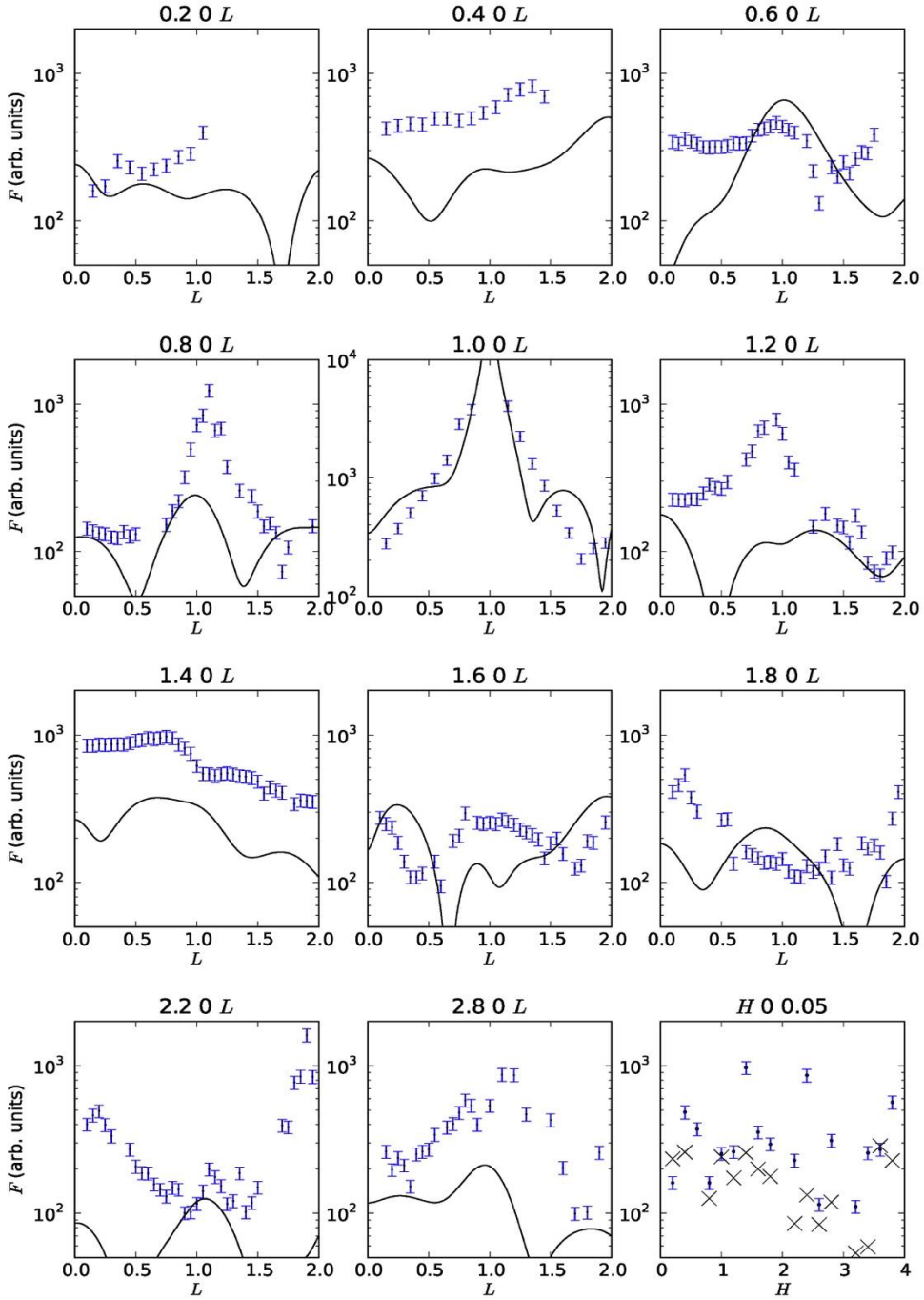

Figure S4. Comparison between the experimental structure factors measured and the theoretical structure factors derived from the stacked dimers model. Blue dots: experiments, continuous black line: simulations.

In Fig. S5 and Table S1 are given the atomic Si and Ag positions refined for the pentamer model that give the best agreement with the GIXD experimental structure factor (see Fig. 4 of the main document for the comparison between experimental and simulated structure factors).

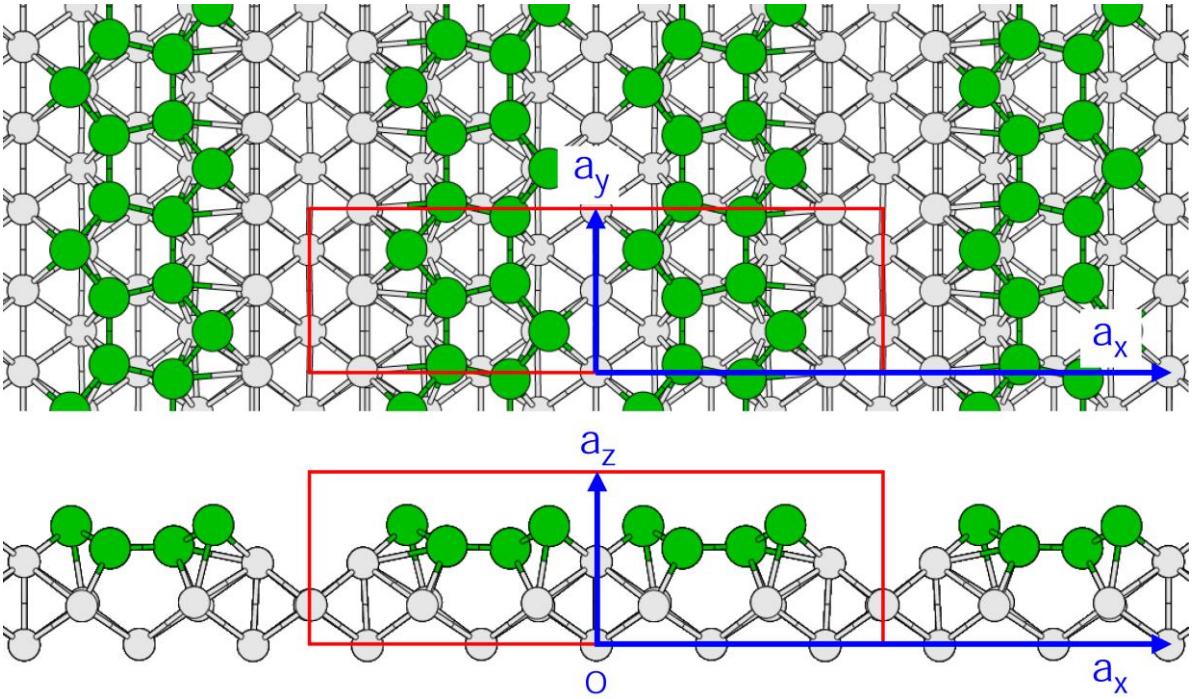

Figure S5. Atomic configuration of Si/Ag(110) pentamers giving the best fit to the GIXD data.

Atom	*x*	*y*	*z*
Si	-0.7766	1.0945	1.2847
Si	-0.7766	1.9055	1.2847
Si	-0.3898	0.5000	1.3959
Si	-1.6331	1.5000	1.4382
Si	-1.2678	0.9072	1.3170
Si	-1.2678	0.0928	1.3170
Si	1.2678	1.0928	1.3170
Si	1.2678	1.9072	1.3170
Si	1.6331	0.5000	1.4382
Si	0.3898	1.5000	1.3959
Si	0.7766	0.9055	1.2847
Si	0.7766	0.0945	1.2847
Ag	2.0741	1.0002	0.9808
Ag	0.0000	1.0000	1.0149
Ag	-2.0741	0.9998	0.9808
Ag	2.0741	-0.0002	0.9808
Ag	0.0000	0.0000	1.0149
Ag	-2.0741	0.0002	0.9808
Ag	2.4443	1.5000	0.4394
Ag	1.4770	1.5000	0.5031
Ag	0.5570	1.5000	0.4830
Ag	-0.4714	1.5000	0.5456
Ag	-1.5760	1.5000	0.5131
Ag	2.5557	0.5000	0.4394
Ag	1.5760	0.5000	0.5131
Ag	0.4714	0.5000	0.5456
Ag	-0.5570	0.5000	0.4830
Ag	-1.4770	0.5000	0.5031
Ag	1.9942	0.9987	-0.0131
Ag	1.0153	0.9808	0.0302
Ag	0.0000	1.0000	0.0297
Ag	-1.0153	1.0192	0.0302
Ag	-1.9942	1.0013	-0.0131
Ag	1.9942	0.0013	-0.0131
Ag	1.0153	0.0192	0.0302
Ag	0.0000	0.0000	0.0297
Ag	-1.0153	-0.0192	0.0302
Ag	-1.9942	-0.0013	-0.0131

Table S1. Atomic coordinates for Si atoms and for the first three Ag atomic planes for the pentamer (5×2) reconstruction. Values are in reduced units with $\vec{a}_x = a\,(0,0,1)$, $\vec{a}_y = a\,(\frac{1}{2},-\frac{1}{2},0)$, $\vec{a}_z = a\,(\frac{1}{2},\frac{1}{2},0)$ where a = 0.4085 nm.

Summary of proposed models

	Pentamers	Zigzag A	Zigzag B	Stacked dimers	Honeycomb
(5x2)/c(10x2)	✓	✓	✓	✓	×
STM	✓	×	✓	×	×
XPS Si(1)/Si(2) ratio (exp: 2:1)	2:1	1:1	1:1	2:1	×
Si coverage (exp.: 0.8±0.2 ML)	1.2	0.8	0.8	1.2	1.5
Ag missing-row	✓	✓	✓	×	×
$\Delta\gamma$(DFT)	0	104	219	34	163
χ^2 (GIXD)	13	33	32	41	38

Table S2. Comparison between the different models proposed for the structure of the Si nanoribbon layer on Ag(110) according to various criteria (rows): superstructure unit cell; high resolution STM observations; presence of a Ag(110) missing row reconstruction; DFT-LDA surface energies $\Delta\gamma$ relative to the energy of the pentamer model for $\mu_{Si} = \mu_{Si}^{bulk}$ (in meV/(1x1) cell); and χ^2 values derived from the direct comparison between DFT results and GIXD. The pentamer model yields the best result across all criteria.

[1] O. Robach, Y. Garreau, K. Aïd, and M. B. Véron-Jolliot, J. Appl. Crystallogr. **33**, 1006 (2000).